Composite Cathode for High-Power Density Solid Oxide Fuel Cells

Final Report

Reporting Period: October 1, 2002 – January 31, 2004

Principal Author : Ilwon Kim

Collaborating Authors : Scott Barnett, Yi Jiang, Manoj Pillai, Nikkia McDonald, Dan Gostovic, Zhongryang Zhan, Jiang Liu

DOE Award Number: DE-FC26-02NT41570

Functional Coating Technology, LLC.

1801 Maple Ave. suite # 5320

Evanston, IL 60201

This report was prepared as an account of work sponsored by an agency of the United States Government. Neither the United States Government nor any agency thereof, nor any of their employees, makes any warranty, express or implied, or assumes any legal liability or responsibility for the accuracy, completeness, or usefulness of any information, apparatus, product, or process disclosed, or represents that its use would not infringe privately owned rights. Reference herein to any specific commercial product, process, or service by trade name, trademark, manufacturer, or otherwise does not necessarily constitute or imply its endorsement, recommendation, or favoring by the United States Government or any agency thereof. The views and opinions of authors expressed herein do not necessarily state or reflect those of the United States Government or any agency thereof.

ABSTRACT

Reduction of solid oxide fuel cell (SOFC) operating temperature will play a key role in reducing the stack cost by allowing the use of low-cost metallic interconnects and new approaches to sealing, while making applications such as transportation more feasible. Reported results for anode-supported SOFCs show that cathode polarization resistance is the primary barrier to achieving high power densities at operating temperatures of 700^{o}C and lower. This project aims to identify and develop composite cathodes that could reduce SOFC operating temperatures below 700^{o}C.

This effort focuses on study and use of (La,Sr)(Co,Fe)O_3 (LSCF) based composite cathodes, which have arguably the best potential to substantially improve on the currently-used, (La,Sr)MnO_3-Yttria-stabilized Zirconia. During this Phase I, it was successfully demonstrated that high performances can be achieved with LSCF/Gadolinium-Doped Ceria composite cathodes on Ni-based anode supported cells operating at 700^{o}C or lower.

We studied electrochemical reactions at LSCF / Yttria-stabilized Zirconia (YSZ) interfaces, and observed chemical reactions between LSCF and YSZ. By using ceria electrolytes or YSZ electrolytes with ceria diffusion barrier layers, the chemical reactions between LSCF and electrolytes were prevented under cathode firing conditions necessary for the optimal adhesion of the cathodes. The protection provided by ceria layer is expected to be adequate for stable long-term cathode performances, but more testing is needed to verify this. Using ceria-based barrier layers, high performance Ni-YSZ anode supported cells have been demonstrated with maximum power densities of 0.8W/cm^2 at 700^{o}C and 1.6W/cm^{2}at 800^{o}C. Ni-SDC anode supported cells with SDC electrolytes yielded >1W/cm^2 at 600 ^{o}C. We speculate that the power output of Ni-YSZ anode supported cell at 700^{o}C and lower, was limited by the quality of the Ceria and Ceria YSZ interface. Improvements in the low-temperature performances are expected based on further development of barrier layer fabrication processes and optimization of cathode microstructure.

TABLE OF CONTENTS

LIST (S) OF GRAPHICAL MATERIALS

I. INTRODUCTION

The reduction of solid oxide fuel cell (SOFC) operating temperature plays a key role in reducing stack cost by allowing the use of low-cost metallic interconnects and new approaches to sealing. Reported results for anode-supported SOFCs show that reducing the cathode polarization resistance is the primary barrier to achieving high power densities at operating temperatures $\leq 700^{o}C$. For example, one prior study of thin-electrolyte SOFCs showed that the low-current cathode interfacial resistance R_I was 70-85% of the total cell resistance from 550-800^{o}C.[i] Thus, there is considerable current interest in alternative cathodes to LSM-YSZ that can extend operating temperature to $\leq 700^{o}C$.

While the search for new cathode materials is valuable, there are known materials that show considerable promise for low temperature applications. In particular, compositions containing $(La,Sr)(Co,Fe)O_3$ (LSCF) have been shown via impedance spectroscopy[ii,iii,iv] to provide far superior performance compared to $(La,Sr)MnO_3$ (LSM) cathodes. For example, low-current polarization resistances measured for LSCF-GDC (GDC = Gd-doped Ceria) cathodes on YSZ electrolytes are $\approx 0.3\ \Omega cm^2$ at 600^{o}C and $\approx 0.03\ \Omega cm^2$ at 700^{o}C. Theoretical studies[v] have indicated that this is due to a combination of higher oxygen surface exchange rates and bulk oxygen diffusion rates; these rates are high enough to allow good performance down to 600^{o}C. Despite these fundamental advantages, there has been little attempt to incorporate these cathodes into anode-supported SOFCs. This is due in part to the potential difficulties with this material. First, LSCF reacts with zirconia (at least for Co-containing compositions) to form resistive interfacial zirconate phases, severely limiting cathode performance. Second, processing temperatures are low enough that progressive sintering during longer-term cell operation may compromise the long-term stability.

The main objectives of this project were to assess cathode stability and develop materials processing methods that optimize the cathode microstructure and performance. Ceria layers were studied as diffusion barriers to provide stability against LSCF-YSZ reactions during processing. Using SDC electrolytes or GDC interlayers between the cathode and YSZ electrolyte, high power densities were demonstrated at temperatures ranging from 600 to 800°C. Screen printing, which is widely used in the SOFC industry, was used for cell fabrication. The effects of microstructure on cathode performance and stability were studied. Material parameters related to the cathode kinetics in LSCF have been measured.

II. EXECUTIVE SUMMARY

Reduction of SOFC operating temperature will play a key role in reducing the stack cost by allowing the use of low-cost metallic interconnects and new approaches to sealing, while making new applications such as transportation more feasible. Reported results for anode-supported SOFCs show that cathode polarization resistance is the primary barrier to achieving high power densities at operating temperatures 700^{o}C or lower.

In this work, we have carried out a feasibility study on cathodes based on (La,Sr)(Co,Fe)O_3 (LSCF). Recent studies of LSCF-based cathodes have shown the potential in obtaining high power densities down to 600^{o}C. The principal problem is that little or no work has been done on anode-supported SOFCs with these materials, thus much work needs to be done to establish the utility of these cathodes. The following is the summary of the work done during this phase I project.

First, symmetric composite cathodes on single crystal YSZ substrates were used to study the electrochemical performance of the LSCF-GDC with and without GDC interlayers. The inclusion of a GDC interlayer typically reduced polarization resistance substantially, e.g. by more than 50% to 0.3Ωcm^2 at 650°C. The reaction between LSCF-GDC and YSZ has been studied using Cross Sectional Scanning Electron Microscope and impedance spectroscopy for symmetric cathode samples, as well as using x-ray diffraction on bulk samples. Basic kinetic data for $La_{0.6}Sr_{0.4}Co_{0.2}Fe_{0.8}O_{3-\delta}$, were obtained using porous LSCF symmetric samples and the Adler-Lane-Steele (ALS) model.

High performance LSCF-GDC cathodes were demonstrated at low temperatures using Ni-SDC anode supported cells with ceria electrolytes, exhibiting power density > 1 W/cm^2 at 600^{o}C. To implement this cathode to a conventional Ni-YSZ anode supported cells, thin GDC interlayers between the YSZ electrolyte and cathode were used to prevent the chemical reaction between LSCF and zirconia. The resulting Ni-YSZ anode supported cells exhibited power densities of 1.6W/cm^2 at 800°C and 0.8W/cm^2 at 700°C. This is considerably higher performance than that of similarly fabricated Ni-YSZ/YSZ/LSM-YSZ cells, 1-1.1W/cm^2 at 800°C and 0.5-0.6W/cm^2 at 700°C. Stable cell operation was demonstrated for >100 hours. The addition of a GDC interlayer allowed an increase in cathode sintering temperature without LSCF-YSZ reaction from ≈900°C to ≈1100°C. . Higher sintering temperature is expected to improve the long-term stability by producing a microstructure that is more stable at cell operating temperature. . More work is needed in the area of long term testing (>>1000hr) or accelerated testing in order to verify the practical stability of the developed cathode approach.

The results of the phase I feasibility study support the potential of LSCF-GDC composite cathodes for a high performance SOFC operating at 700°C or lower. Remaining work include the demonstration of a long-term stability of the cells and obtaining higher performance at 700°C in the case of Ni-YSZ anode supported cells with GDC interlayers. Improvement in performance is expected based on the optimization of the GDC interlayer processing as well as the microstructure of the cathodes.

III. EXPERIMENTAL

1. Preparation of $La_{0.6}Sr_{0.4}Co_{0.2}Fe_{0.8}O_3$-$Ce_{0.8}Gd_{0.2}O_3$ (LSCF-GDC) Powder

A 100g batch of 50:50 wt% LSCF-GDC powder were attrition milled in ethanol to achieve good mixing between LSCF and GDC powders. Attrition milling was carried out to obtain similar particle sizes and thus reduce the particle size distribution in the powders. After milling, the slurry was dried in air @150C/5hrs. The dried powder was then dry milled ~30 hrs to prevent the calcination of any powder agglomerates present after attrition milling.

After dry milling, four 20g-powder batch samples were calcined at 650°C/3hrs, 750°C/3hrs, 850°C/3hrs and 950°C/3hrs respectively. These powders were calcined to promote stability and control shrinkage during cathode sintering. After calcining, the powders were dry milled ~30hrs again to break up any agglomerates that may have been formed as particles grew during calcination. Particle growth and pore size as a function of calcination temperature was also examined. Obtaining a homogeneous distribution of LSCF and GDC was the goal.

For non-calcined powder, 50g batch of 50:50 wt% LSCF-GDC powder was wet ball milled in CH_3O_3 overnight to achieve good LSCF-GDC powder mixing. The slurry was then dried in air @150°C/5hrs. The dried powder was then dry milled ~30 hrs to further break up agglomerates.

2. Screen printing

LSCF-GDC Cathode Layers

All cathode inks prepared from both calcined/non-calcined powder were mixed with vehicle using a 3-roll mill. Initial viscosities for calcined INKS 650, 750, 850 and 950 that correlated to higher solids loading were too thick for printing. Vehicle was added to all of these ink sets reducing the solids loading by volume to 10%, 21%, 18% and 17% respectively. Powders prepared at the lower calcination temperatures have a higher surface area requiring more vehicle to coat the particle surface resulting in lower solids loading. Higher calcination temperatures allow for more particle growth yielding larger sized particles enabling the particle surfaces to be coated with less vehicle. Thus this condition was used all work afterwards.

Triple layers of LSCF-GDC were screen printed onto both sides of a double sided, single-crystal YSZ substrate. Different mesh count screens were used to obtain the desired print thickness after sintering. The cathodes were sintered at temperatures ranging from 900°C-1025°C for 3 hrs. Scratch tests showed an increase in LSCF-GDC adhesion to YSZ with increasing sintering temperature. The LSCF-GDC post sintered layer thickness ranged from ~12 µm to ~ 22 µm, layer roughness ranged from ~ 2 µm – 7 µm.

GDC interlayer

GDC inks were prepared from as-received calcined GDC powder having average particle sizes of ~.8μm and ~.2 μm respectively. The powders were mixed with vehicle using a 3-roll mill. The solids loading by volume of these inks was 20% and 13%.

3. Symmetric cathode preparation and Impedance Measurement

Double sided, polished, single crystal YSZ substrates were "sanded" with 240 grit SiC paper (Rq ~ .4 μm) to roughen the substrate surface for improved adhesion between the cathode layers and the substrate. The LSCF cathodes were initially spray coated using conventional spray pens, due to previous success in using this technique for cathode and electrolytes. Typical impedance scans were conducted at 50°C intervals from 800-450°C. Fifteen minutes were allowed to stabilize at each plateau and then the scan was taken. The impedance scan frequencies were from 0.1-10E^6 Hz. The voltage amplitude was 0.03V. The number of points that were plotted was 120. The impedance data was graphed on the real vs. imaginary axis with Z'(Ω-cm^2) being real and –Z"(Ω-cm^2) being imaginary.

4. Accelerated testing

After the samples were sintered for 1025°C for 3 hours or 900°C for 3 hours, depending on particle sizes, platinum grid was fitted to the cathode area and the leads coming from the samples were looped around the platinum mesh to create a mechanical contact. The platinum mesh was then hand painted over with the appropriate cathode conducting layer, with the leads being wrapped around. The samples were then fired at 1025°C for 3 hours or 900°C for 3 hours, sintering the cathode layers together through the mesh.

After sample preparation, the samples were placed in the furnace. The furnace temperature was then ramped up to 450°C and IS scans were conducted from 450°C to 850°C at 50°C intervals. After the first 850°C IS scan, the IS scan was repeated over dwell time ranging 12 hours to 24 hours.

5. Anode supported cell fabrication, cell testing and Cr contamination test.

NiO-YSZ (1:1wt) pellets were prefired at 1000°C for 4 hours, YSZ was coated on the NiO-YSZ pellets by colloidal method and screen printing and then sintered at 1400°C for 4 hours. After co-firing LSCF-GDC (1:1wt) was screen printed on the electrolyte and sintered at temperature ranging 900 – 1100°C for three hours. Another layer of pure LSCF was screen printed on top of the LSCF-GDC layer and sintered at 900 – 1100°C for 3 hours.

LSM-YSZ cathode: LSM-YSZ (1:1wt) was screen printed on the electrolyte and fired at 1100°C for 3 hours. Then, another layer of pure LSM was screen printed on top of the LSM-YSZ layer and sintered at 1100°C for 3 hours.

In order to verify the effect of Cr-poisoning of the cathode from stainless steel, a thin piece of 300-series stainless steel was attached to the cathode part of both cells (LSM and LSCF) using silver paste (picture below).

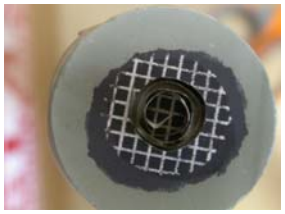

Figure 1. A picture of set-up for Cr contamination cell tests, showing stainless steel attachment in contact with cathodes.

III. RESULTS AND DISCUSSION

TASK 1: ELECTROCHEMICAL MEASUREMENTS ON SYMMETRIC CATHODE STRUCTURES

The $La_{0.6}Sr_{0.4}Co_{0.2}Fe_{0.8}O_{3-\delta,}$ powders with a particle size less than 500nm was used for spray coating LSCF cathodes on single crystal YSZ substrates YSZ substrates were used due to unavailability of GDC single crystal substrates. According to our previous work, use of single crystal substrate is desirable for the interpretation of resulting impedance arc, since large arc originating from grain boundary interface of thick electrolyte often overlapped the arc from cathode / electrolyte interface. The surface of YSZ substrates was roughened to simulate the interface property of typical cell. The RMS roughness used for the substrate after treatment was in range of 200nm - 1 micron. The spray coated LSCF turns out to be porous according to the SEM micrograph, since the sintering temperature was selected to be relatively low to avoid a potentially severe reaction between LSCF and YSZ. Consequently, we used Adler-Lane-Steel (ALS) model[vi] for the porous cathode instead of equivalent circuit model, which generated reasonable initial data on oxygen diffusion co-efficient and surface exchange rates for LSCF as described below.

Figure 2 shows the microstructure of spray coated LSCF layers. A relatively porous structure of layer is evident with clear interface between LSCF and YSZ substrates. Average porosity and particle size values were estimated from a number of cross sectional SEM images of LSCF layers, to be ~ 30% and ~ 300 nm respectively.

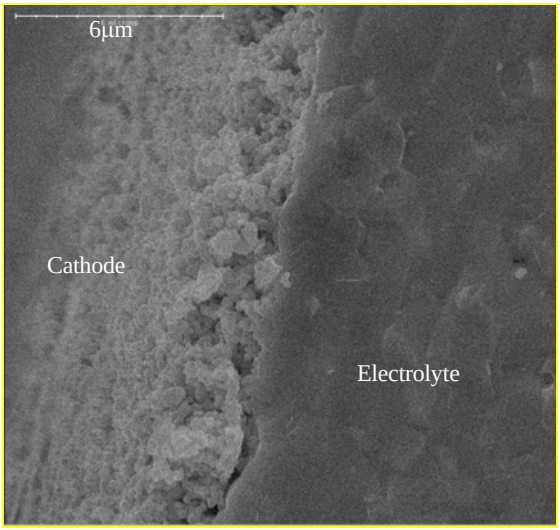

Figure 2. SEM micrograph on porous LSCF layer spray coated on an YSZ single crystal substrate.

Impedance arcs from EIS (Electrochemical Impedance Spectroscopy) characterization has been studied with ALS model, that takes into account the fact that for a mixed ionic conductor such as LSCF, the reaction zone extended beyond three-phase boundaries. In this case, with an infinitely thick layer boundary condition, chemical resistance is expressed as following,

$$R_{chem} = (RT/2F^2)[\tau/(1-\varepsilon)aC_o^2D^*k]^{1/2}$$

where following are values for parameters used above. Note that the porosity was estimated based on the cross section SEM micrograph and the surface area was estimated from average particle size from SEM with assumption of sphere shaped particle.

τ = tortuosity = 1.5

ε = fractional porosity = 0.3

a = surface area/volume = 20,000 cm-1

C_0 = oxygen concentration = 0.09 mol cm-3

D* = oxygen bulk diffusion coefficient

k = surface exchange coefficient

Thick LSCF films (30 micron) should be appropriate for this model. Figure 3 shows a typical impedance arc measured at 650 °C, from LSCF /YSZ samples with fittings based on ALS model. The fitting provided a relatively good agreement with ALS model with estimated bulk diffusion coefficient and surface reactivity of D* ~ $1x10^{-8}$ cm^2/s and $k\sim1x10^{-5}$, in general match with some of pervious data on LSCF [vii] and is in reasonable value compared to data found for similar materials like LSC.[vi] However the accuracy of fitting was limited by the high frequency arc interfering left hand side of arc and further study for this value will be conducted as described above. The source of high frequency arc is unclear.

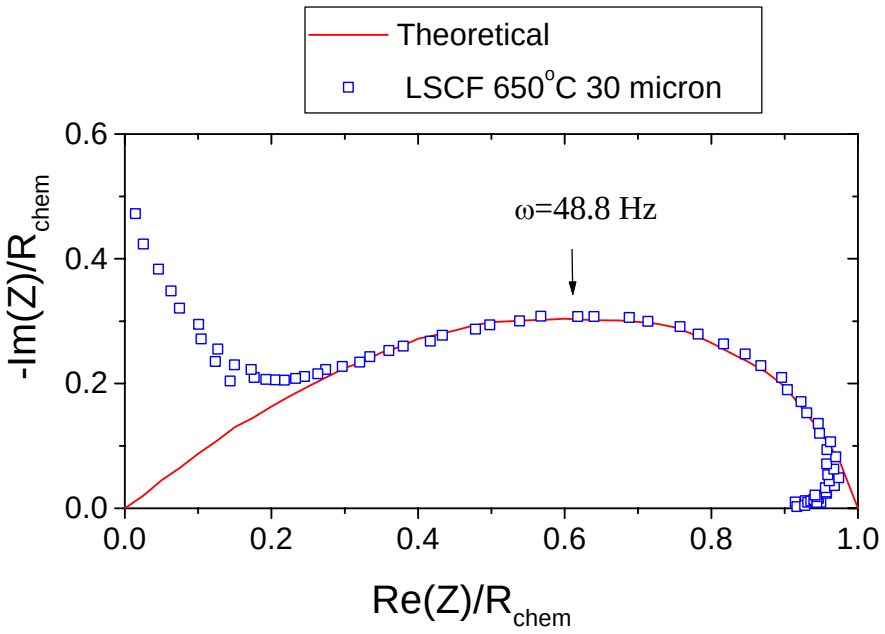

Figure 3. A typical experimental impedance arc from LSCF /YSZ samples with fitted curve based on the ALS model.

TASK 2. LSCF-YSZ REACTION

Originally following works were proposed:

i) XRD, and cross-sectional SEM: observe reaction layer for different LSCF compositions
ii) Impedance spectroscopy: measure interfacial resistance.
iii) Model the reaction kinetics.

At the start of phase I, portion of this task has been reduced based on the suggestion from the proposal review.

LSCF/YSZ reaction was observed, using X-ray diffraction, in the LSCF-YSZ pellets with LSCF particle size less than 500nm, when the pellets was sintered at 1025°C for 3 hours. The reaction product was identified as $(Sr,Zr)O_3$, in agreement with some previous studies.[viii,iii]
Based on the comments from SECA core team review, a detailed LSCF –YSZ reaction study has not been conducted during this Phase I. Instead, more focus was given to GDC interlayer development.

Task 3. EFFECT OF INTERFACIAL LAYERS

- Task 3.1 Screen printing and microstructure characterization of LSCF-GDC on YSZ

Initially, LSCF-GDC screen printing ink formulation and microstructure control via powder processing were conducted The purpose of this work ultimately was to find the optimal microstructure, in terms of particle size, size distribution, particle connectivity porosity and adhesion to the YSZ, such that the cathode will have high activity as well as long term-stability. Among other microstructure related parameters, it is in general, expected that the smaller particle size would be favorable for a higher activity of the electrode, while for a long-term stability, coarsened particle would be favorable, assuming that other factors are ideal. We assume that there will be some median region where both of performance and stability would be acceptable. To eventually find this optimal point, initial work consisted of attrition milling as received LSCF and GDC after mixing, reducing the particle size and subsequently calcining the powder to varying temperatures to obtain different desired particle sizes. However, other parameters effected the microstructure of the cathodes, including the variation of screen ink quality such as ink rheology, viscosity, solid loadings as well control of the agglomeration of the particle within the ink, all of which was a function of particle size among other factors. As the results, the optimization of cathode microstructure entailed a large parameter space for Phase I time frame. Most of this work done were during the earlier stage before the optimization process to screen printing the GDC interlayer, so they were limited to the composite cathodes directly on YSZ.

The calcining temperature of LSCF-GDC powder after attrition milling was varied from 650°C to 1100°C. Although all condition resulted in non-ideal particle size

distribution and structure having some amount of agglomeration according to SEM micrographs, the 850°C calcined powders showed the best particle structures. Thus calcining temperature of 850°C was used for the LSCF-GDC samples during the rest of Phase I. The screen printing ink was made using the calcined powder and printed cathodes were fired at temperatures ranging between 900°C to 1000°C. Figure 4. shows typical impedance arc from LSCF-GDC symmetric cathode layer deposited on YSZ substrates without GDC interlayer. The arc shape appears "Gehrischer"-type arc at lower T, while it become symmetric at higher T, suggesting strong T dependence of impedance value agreeing with prior work.[iv] In the previous work using spin coating, the low frequency arc was dominating under 700°C, indicating the rate-limiting step may be a diffusion related process.[iv] Here, the size of the arcs overall, are substantially larger and the high frequency arc is comparatively larger than that of low temperature ones, except for those at 650°C. This may have to do with the higher cathode sintering temperatures used for this study compared to that used for previous one. The higher temperature was required for the adequate adhesion of the samples when screen printing was used and may have contributed to deterioration of the interface between cathode and YSZ due to a reaction.

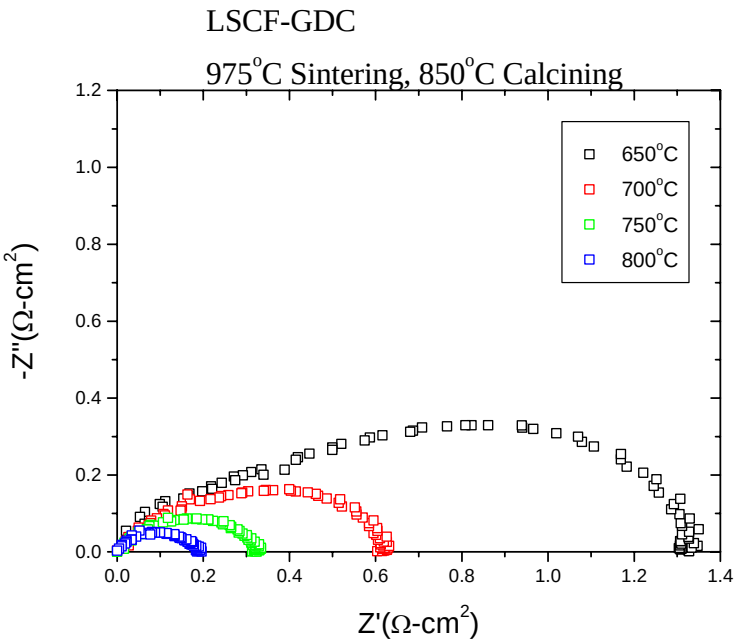

Figure 4. Typical impedance arcs from a symmetric LSCF-GDC cathode layer deposited on an YSZ substrates without a GDC interlayer.

Figure 5 shows the interfacial impedance dependence of LSCF-GDC symmetric cathode vs. sintering temperature of cathodes varying from 925°C to 1100°C. The effect of sintering temperature is clear with impedance decreasing as the sintering temperature increases, reaching a minimum impedance of 0.6 Ω at 700°C and 0.17 Ω at 800°C for sintering temperature of 1025°C. While this value is substantially higher than that of the previous work, it seems to be limited by LSCF-YSZ reaction as well as non-optimized

microstructure in the active reaction surface area. It may be possible that the particle size of the starting powder after attrition milling have been too small in such that agglomeration was not complete controlled and adversely effected on obtaining the optimal microstructures. Further increase in sintering temperature increased impedance reaching ~3.5 Ω cm^2 at 1100°C. This is likely due to sintering of pore structure as well as extensive reaction between LSCF and YSZ. The initially optimized sintering temperature for calcined cathode layer is about 100°C higher than previous optimized sintering temperature for finer particles. Note that the slope changes for sintering temperatures over 1025°C, indicating that the rate-limiting factor might be changing for higher temperature sintered samples. Whether this is due to pore closing by sintering or more severe LSCF-YSZ reaction is not clear.

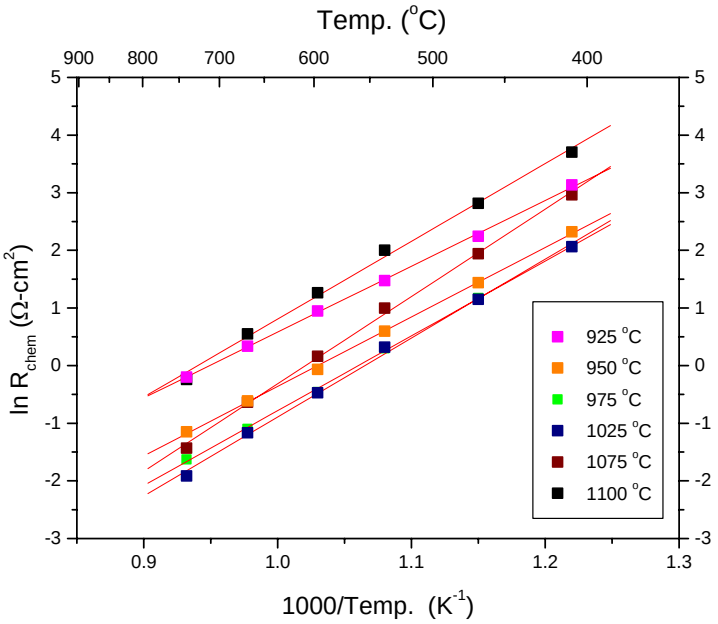

Figure 5. Polarization resistances of LSCF-GDC symmetric cathodes without a GDC interlayer shown with respect to the cathode sintering temperatures varying from 925°C to 1100°C.

Figure 6 shows a cross sectional SEM image from an 850°C calcined, 950°C sintered cathode. While this condition exhibited the best particle size and structure distribution based on SEM on raw particles, the sintered cathode microstructure appeared needing further optimization. As can be seen in the figure 6, the adhesion between cathode and YSZ appears to be not very complete and the pore structure may not be as well connected as previous spin coated cathodes.

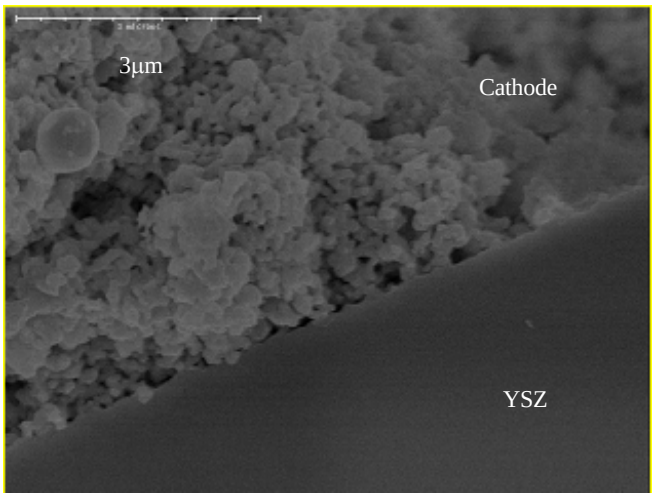

Figure 6. Cross sectional SEM images from screen printed LSCF-GDC cathodes fired at 950°C, using powders calcined at 850°C.

Figure 7 compares impedance values at 700°C for symmetric cathodes of (a) porous LSCF on GDC polycrystalline electrolyte, (b) porous LSCF on YSZ single crystalline substrate and (b) porous LSCF-GDC composite cathode on YSZ single crystal substrate. The composite cathode clearly shows order of magnitude lower impedance compared with LSCF cathode probably due to reaction zone extending beyond the triple phase boundaries. The impedance arc from LSCF on GDC was substantially larger than that from LSCF on YSZ substrate, but it is not clear whether this large arc originate from the grain boundaries in the polycrystalline GDC substrate or GDC/LSCF interface. All three samples were sintered at 900°C.

Porous LSCF on GDC polycrystalline electrolyte	Porous LSCF on YSZ single crystal electrolyte	Porous LSCF-GDC on YSZ single crystal electrolyte

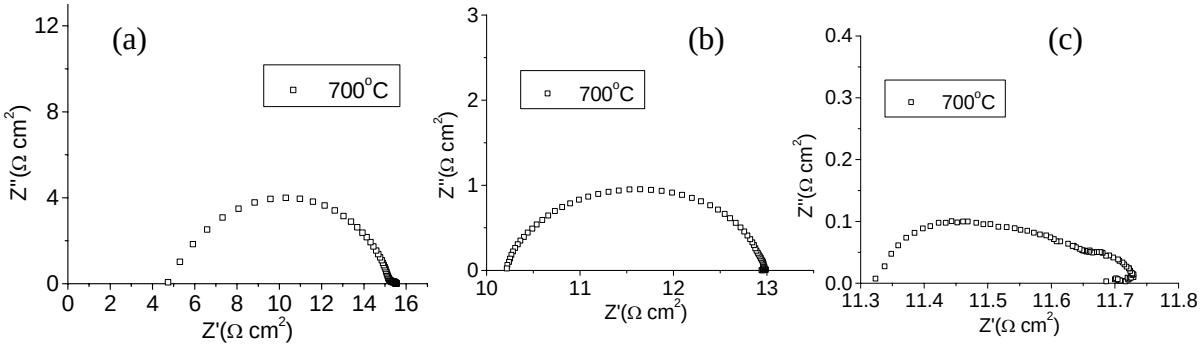

Figure 7. Impedance arcs at 700°C for various cathode/electrolyte combination (a) A porous LSCF on a GDC polycrystalline electrolyte supports, (b) A porous LSCF on a YSZ single crystalline supports and (c) A porous LSCF-GDC composite cathode on a YSZ single crystal substrate.

For LSCF-GDC cathode, ball-milled mixture of as-received LSCF powder and GDC powder was used and the cathode samples were sintered at 900°C. The impedance value of 0.4 Ω cm^2 at 700°C is better than the best value of calcined powder and is presumably due to larger reaction area resulting from smaller particle size (<< .5 micron). However, when fabrication method was changed to screen printing with same powder, the impedance increased to 1 Ωcm^2 at 700°C, indicating the need for further optimization of the screen printing ink. When the sintering temperature increased to 950°C, the impedance value at 700°C further increased to 2.5 Ωcm^2, may be suggesting more reaction problem with YSZ electrolyte. The screen printed layer with calcined powder instead of the as received smaller particle size powder exhibited approximately 100°C higher optimum sintering temperature for obtaining their lowest impedance over different temperatures. This may suggest that the microstructure coarsening improves the stability of LSCF-GDC against sintering as expected. On the other hand, relatively simple impedance spectroscopy currently being used cannot distinguish the increase in impedance due to sintering or surface solid state reaction between cathode and electrolyte and this limits a better analysis.

Figure 8 shows cell testing results on anode-supported cell with LSCF-GDC cathode without GDC interlayer. The button cell consists of Ni-YSZ support with YSZ electrolyte fabricated using colloidal methods. Power density was 0.6 W/ cm^2.

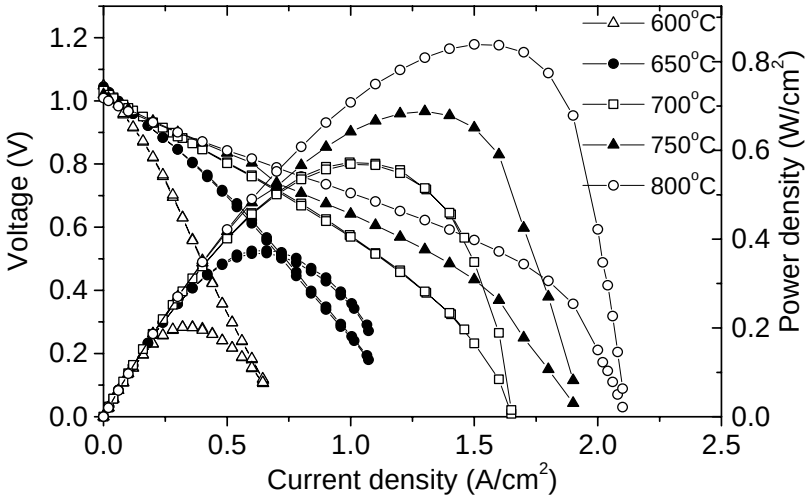

Figure 8. Cell test results on anode-supported cell with LSCF-GDC cathode without GDC interlayer. The button cell consists of Ni-YSZ support with YSZ electrolyte fabricated using colloidal methods.

The power density correlated somewhat with impedance during the cell operation. Figure 9 shows (a) the impedance arc from anode supported cell under H_2 at open circuit voltage condition and (b) current flowing condition. The cathode part of arc was simulated using ALS model and superimposed with experimental curves. The figure 9 (a) shows cathode related impedance on the right hand side arc in range of ~ 0.17 Ω cm^2 at 700°C at open circuit voltage condition. The arc on the left hand side changed when the fuel was switched, thus we believe the right hand side arc is responsible for the cathode /electrolyte interface. While this value is substantially lower than that of symmetric cathodes with both calcined and as-received powder, it is still much higher than value, 0.03 Ω cm^2 at 700°C from cathode previously spin coated at Northwestern University. Probably the LSCF-YSZ reaction is limiting the impedance. Figure 9 (b) exhibits the impedance arcs from anode-supported cells with cathode fabricated similarly, comparing in current flowing condition. The cathode impedance is 0.07 Ω at 700°C, with current density of 0.4A/cm^2, substantial reduction in the impedance under current flowing condition is consistent with previous observations.

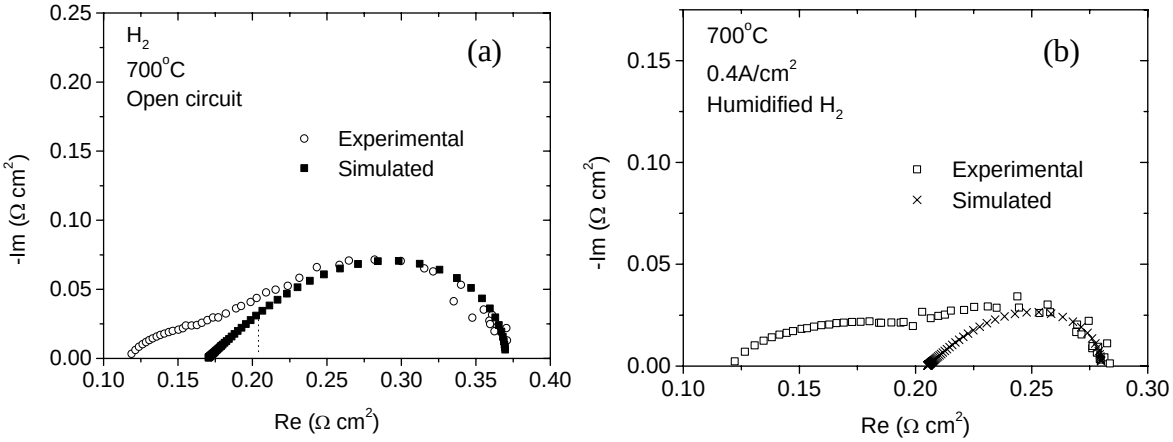

Figure 9. Impedance arcs from a Ni-YSZ anode supported cells with a LSCF-GDC cathode and a YSZ electrolyte, comparing under (a) open circuit condition and (b) current flowing condition.

A preliminary stability test for the anode-supported cell was done under methane fuel. The LSCF-GDC cathode was stable over 100 hours of operation under humidified methane at operation under 700°C. (Figure 10) While this is reasonable data, further longer term testing or accelerated testing should be conducted in much longer time scale.

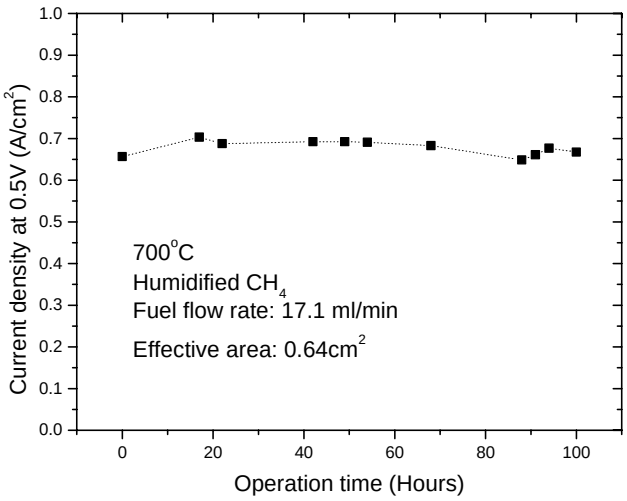

Figure 10. Results of a preliminary stability test on Ni-YSZ anode/YSZ electrolytes/LSCF-GDC cathode cells.

- Task 3.2 Ceria based interlayer fabrication and testing of cell with GDC interlayer layers.

The substantially high impedances of LSCF-GDC cathode on YSZ substrates compared suggest the chemical reaction between YSZ and LSCF during the cathode sintering stage. Subsequent study on LSCF-GDC /YSZ symmetric samples, using SEM Energy Dispersive Scan (EDS) Analysis indicated that increased presence of Sr and La in LSCF-GDC interfaces near YSZ. This suggests that these components may diffuse into the interface and form a resistive phase with Zirconia, there by decrease electrochemical performances. Consequently, the development of ceria diffusion barrier layer was identified as the key task on this phase I.

For fabrication of GDC interlayer, screen printing was chosen for their immediate applicability to some SECA core team members. A substantial optimization on the screen printing process was done to obtain thin (< 5 micron), dense GDC interlayer on YSZ single crystal. Primary difficulties included making dense layer from screen printing that is likely to shrink upon sintering on bulk substrate that is already sintered. Also adhesion problem arising from the above mentioned shrinkage issue also was problematic.

Figure 11 compares polarization resistance at different temperatures for LSCF-GDC cathode with and without GDC interlayer, Both samples was fabricated with same parameter except the GDC interlayer, which were fired at 1400°C prior to the composite cathode deposition. Composite cathode powder calcined at 850°C was used and the cathodes were fired at 950°C for both samples. The resistance is at 650 °C with and without GDC are 0.3Ωcm^2 and 0.7Ωcm^2, respectively. These results clearly indicate the effectiveness of GDC interlayer as a reaction barrier, resistance being about half with GDC compared to without GDC interlayer. The slopes of the graph with inverse T were same for

both samples indicating that the ceria interlayer did not have any effect on the rate-limiting step.

Subsequently, an initial SEM EDS study was performed for the symmetric cathode sample with GDC interlayer, where there were no Sr or La detected in the interface between GDC and YSZ, and no increase in Sr and La concentration in LSCF near the LSCF-GDC / GDC interface. This, combined with the polarization resistance measurement suggests that the GDC interlayer is effectively prohibiting the diffusion of these species and prevent the potential formation of resistive phases.

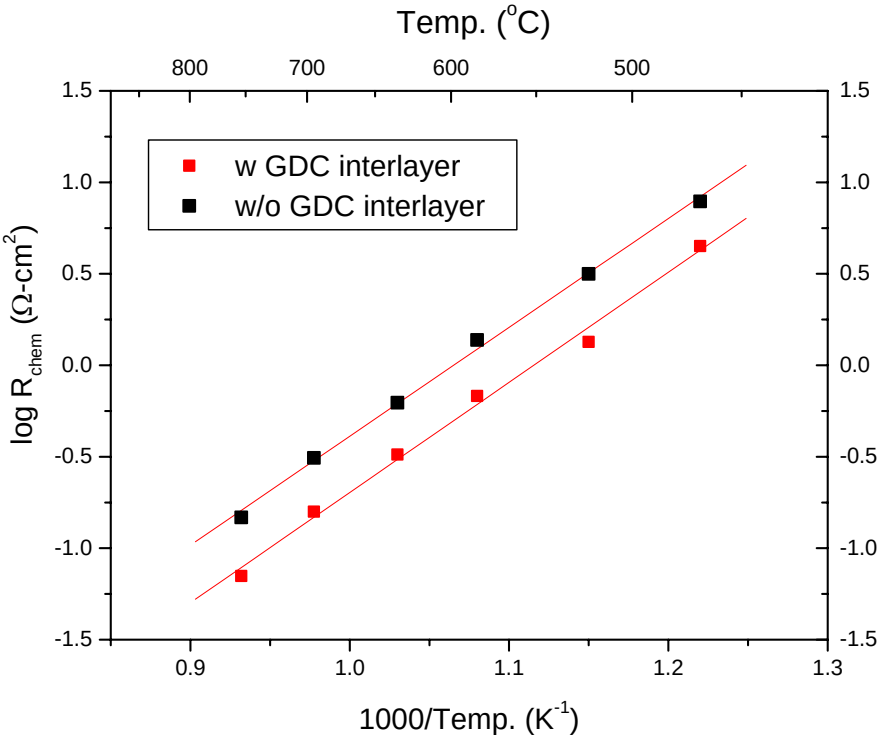

Figure 11. Polarization resistances of the symmetric LSCF-GDC cathodes with and without GDC interlayer shown in relations to the inverse temperatures.

Based on symmetric cathode results with GDC interlayer, we have proceeded with the demonstration of the cathode in anode supported cells. First we have demonstrated that LSCF-GDC can be used for high performance Solid Oxide Fuel Cell with Ni-SDC anode supported cell and SDC electrolyte at low temperature. This approach was chosen to provide baseline for the performance of LSCF-GDC cathode at low temperatures without the potential issues related to the fabrication of GDC interlayer, while substantial process development is on going for screen printing of GDC interlayer using co-sintering with Ni-YSZ anode supports and YSZ electrolytes.

A colloidal method was used to fabricate the Sm-doped ceria layer on dry pressed Ni-SDC (50wt% NiO-50wt% SDC) anode supports and co-sintered at around 1400°C. After

the sintering, LSCF-GDC cathodes were screen printed and 2 layers of LSCF current collecting layer followed the composite cathode.

Figure 12 shows IV curves from dry pressed Ni-SDC/Sm-doped Ceria/LSCF-GDC cathode. An excellent power density of > 1W/ cm^2 was obtained at 600°C, which is higher performance than almost any other previous SOFC performance at this temperature. Such a high power density normally is associated with > 700°C. Power density at higher temperature degraded due to electronic conductivity of SDC. In fact, the open circuit voltage at 600°C on this cell was only ~ 0.9V.

These power densities correlated well with cathode impedance as well. Figure 13 shows the impedance arc from the cell at 623°C where the cathode / electrolyte arc showing only 0.16 Ω cm^2 and was primarily associated with the electrodes, particularly the LSCF-GDC cathode. Because of the high conductivity of SDC and the low thickness (≤10μm), the electrolyte resistance was small down to ≤500 ^oC.

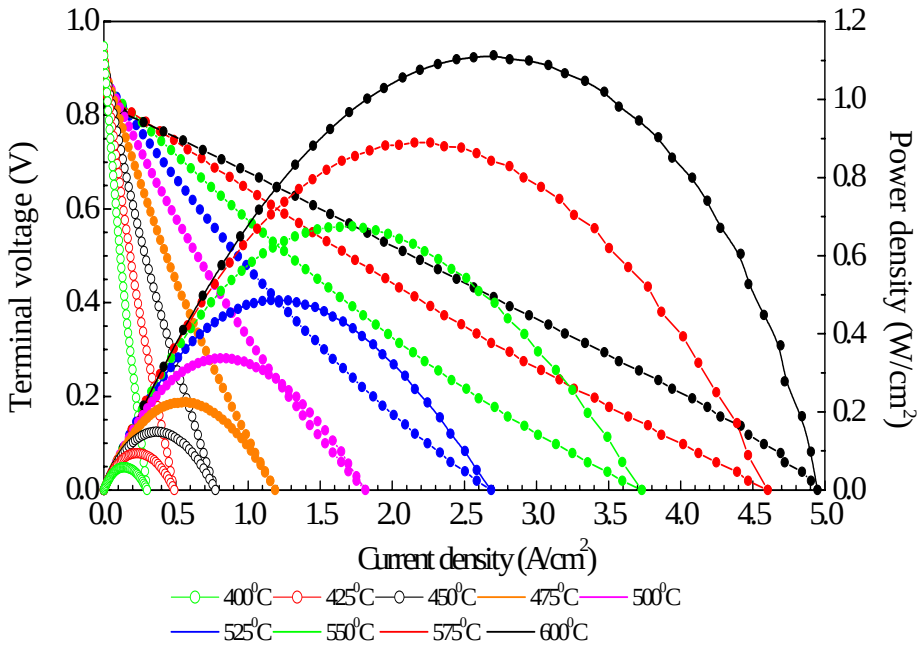

Figure 12. Voltage and power density vs. current density at different temperatures are shown for a Ni-SDC|SDC|GDC-LSCF|LSCF cell. Humidified H_2 and air were supplied.

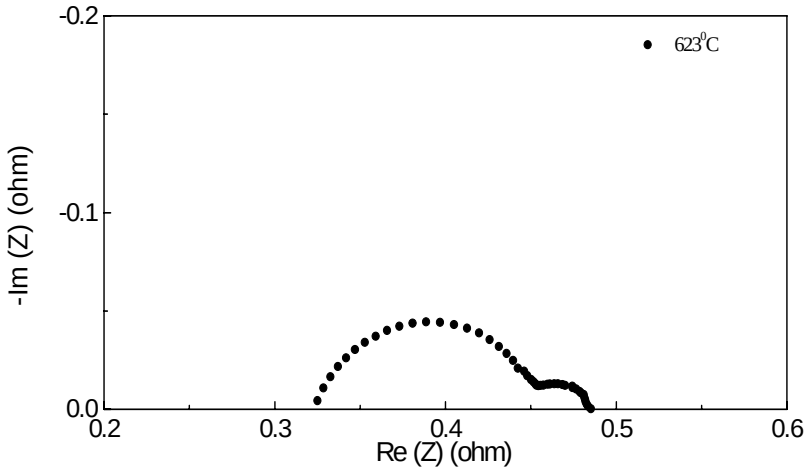

Figure 13. An impedance arc from a Ni-SDC | Sm doped Ceria electrolyte | LSCF-GDC |LSCF |LSCF at 600°C.

Based on the benchmark performance set by Ni-SDC anode supported cells using LSCF-GDC cathodes, more conventional NiO-YSZ supported cells with LSCF-GDC cathodes was developed along with GDC interlayer.

The anode supported cells were multiple layered in structure, consisting of NiO-YSZ anode substrate, NiO-YSZ anode active layer, YSZ electrolyte and SDC interlayer, LSCF-GDC cathode active layer and cathode current collecting layers. NiO-YSZ substrates were die-pressed pellets from 70wt% NiO-30wt% YSZ powder mixture and pre-fired at 1000°C for about 1 hour. The porosity of the anode substrates was modified by adding pore former, such as carbon powders or starch. NiO-YSZ active layers consisted of 50wt% NiO-50wt%YSZ, which was deposited by screen printing. The thickness of the active layer was approximately 20 μm.

The electrolyte and interlayer were prepared by screen printing consecutively YSZ and SDC or GDC layers and fired at 1400°C for 2 hours. The estimated thickness of YSZ and SDC were approximately 6 μm and 5 μm, respectively.

50wt% LSCF-50wt% GDC and pure LSCF were used as the cathode active layer and the current collecting layer, respectively. Both layers were screen printed one after another on top of the interlayer surface and then fired at different temperatures. The SDC or GDC interlayer allowed firing of composite cathode and conduction layer substantially higher temperature (~1100°C) than that were done without the interlayer (900-950°C), allowing better adhesion and potentially higher long-term stability. Fabricated cells were tested using the test fixture with pressure contact between the current collectors, the electrodes and pressure seal.

After the cell was properly assembled, the temperature was brought to 800°C at a typical ramp rate of 10°C /min under a continuous flow of H_2. At 800°C, the cell was *in-situ* reduced for several hours to ensure complete reduction of NiO to Ni for optimal porosity and conductivity. After reduction and stabilization, the cell performance was evaluated under a H_2 flow rate of 100 ml/min and an airflow rate of 500ml/min. I-V curves were taken at various temperatures. The cells were also analyzed by impedance spectroscopy to determine the ohmic and electrode polarization resistances.

Figure 14 shows performances of a cell fabricated as above at various temperatures. As shown in Figure 14a, OCVs are close to the theoretical values corresponding to air on the cathode side and 3% H_2O- H_2 fuel on the anode side. It increases with decreasing temperature. The maximum power density at 800°C, 700°C and 600°C were about 1.6 W/cm^2, 0.8 W/cm^2 and 0.25 W/cm^2 (Figure 14b), respectively. Impedance analysis results are shown in Figure 15. At 800°C, the ohmic resistance was about 0.13 Ωcm^2, while the total electrode resistance including the anode and cathode was about 0.17 Ωcm^2. At 700°C, they are 0.26 Ωcm^2 and 0.215 Ωcm^2. At 600°C, they were 0.8 Ωcm^2 and 0.6 Ωcm^2. When the temperature dropped from 800°C to 700°C, the increase of ohmic resistance dominated the increase in the area specific resistance. This suggests that the polarization resistance of the cathode is not a factor limiting performances at 700°C. Considering the typical ohmic resistances of YSZ electrolyte at 700°C as well as the thickness of the electrolyte, it has been speculated that the interface between ceria and YSZ may provide a source of additional ohmic resistances. This probably suggests the needs of a substantial improvement on ceria/YSZ interfaces. It is expected that the optimization of interface quality by further development of screen printing process could considerably improve the performance of these cells at 700°C. Note that the IV curves and power density curve was taken up to current of about 3.5A due to the power supply limitation of the cell testing set-up used.

~100hr tests were done to obtain a preliminary assessment on the stability of these cells at 800°C. While the power density typically decreased by 10% or so initially during the testing, subsequent results showed stable performance up to ~100hrs. Further work is necessary to assess long-term stability of these cells, particularly at 700°C.

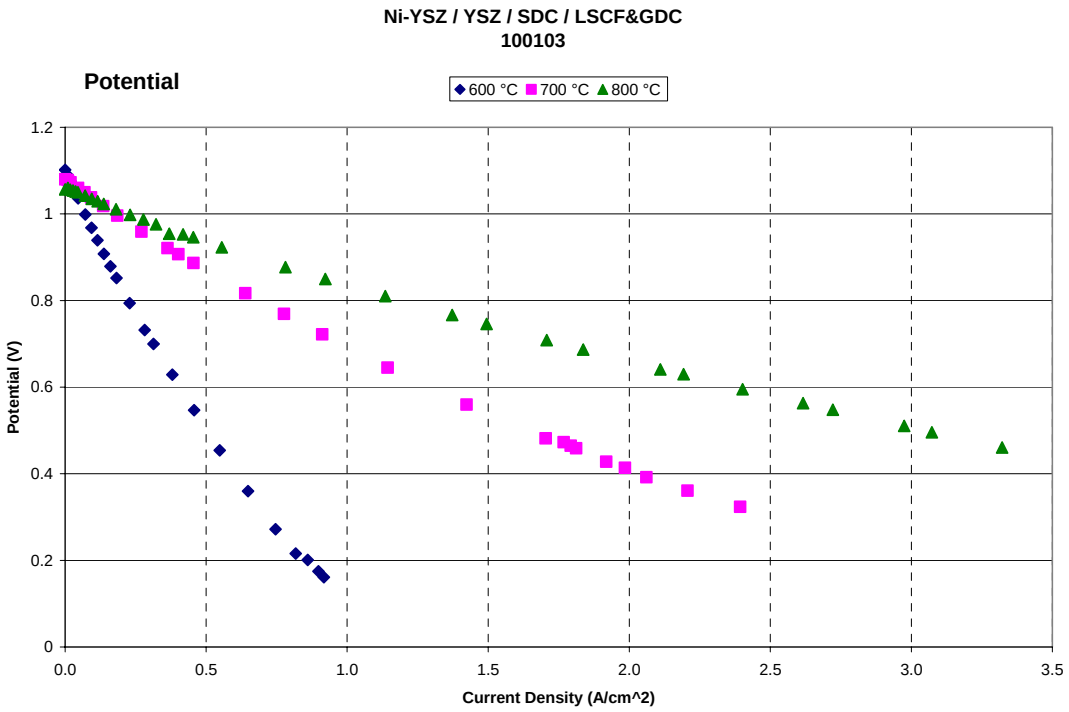

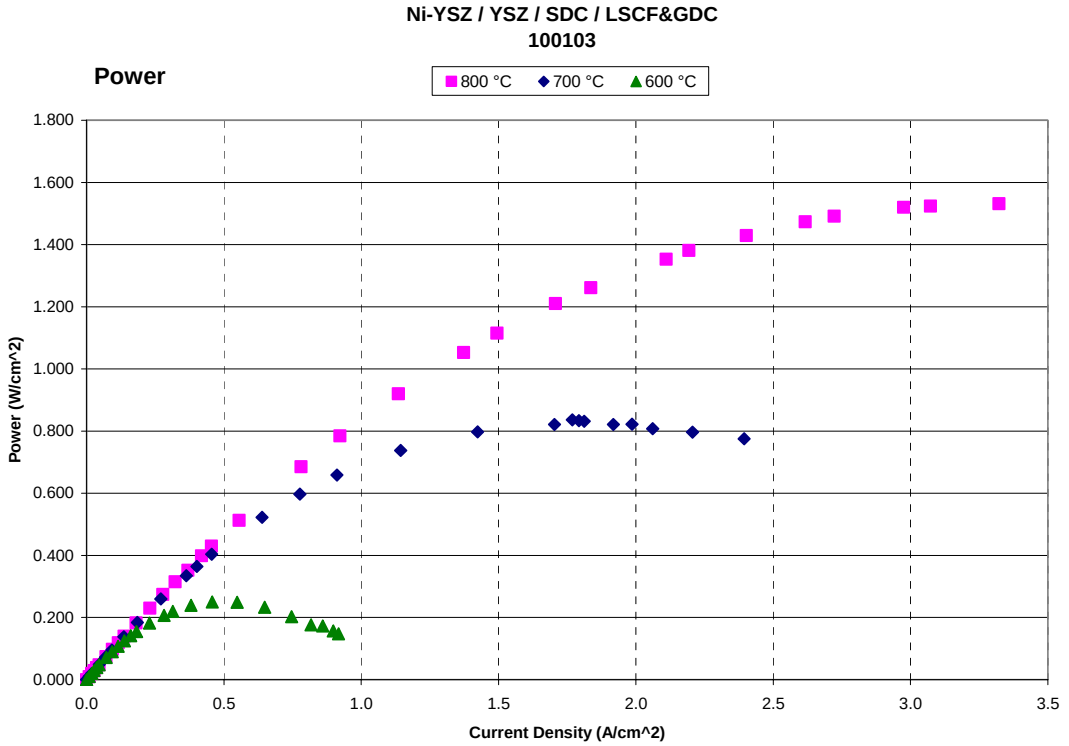

Figure 14 a) IV curve for Ni-YSZ anode supported cells with YSZ electrolyte, SDC interlayer and LSCF-GDC/LSCF cathodes. B) Power density vs. current density plot for the above cells.

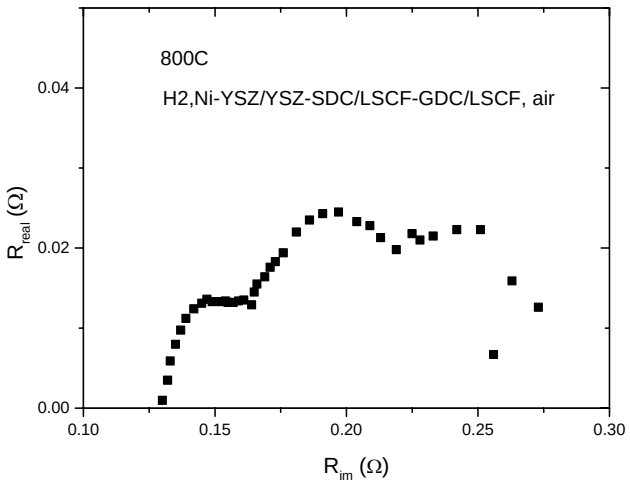

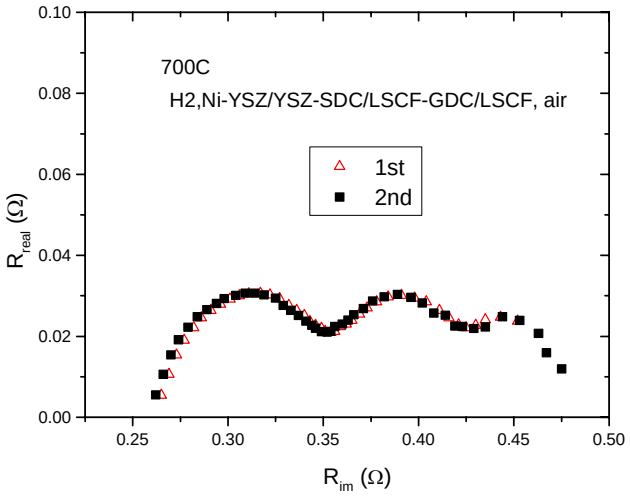

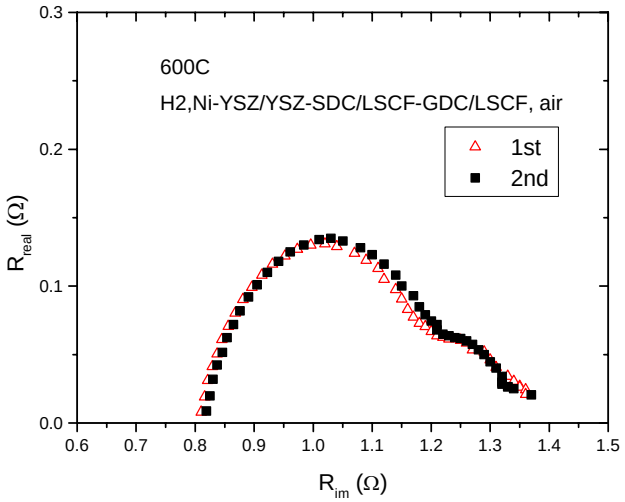

Figure 15. Impedance spectroscopy results at different temperatures for a Ni-YSZ anode supported cell with a YSZ electrolyte, a GDC interlayer with a LSCF-GDC/LSCF/LSCF cathode.

– Task 3.3 Accelerated testing.

A preliminary trial of accelerated testing was done. In this test, the polarization resistances of symmetric composite cathodes were monitored for different LSCF-GDC cathode particle size and with and without GDC interlayer. The range of temperature being studied for this accelerated testing is between 950°C and 1100°C. The purpose of this preliminary experiment was to evaluate the new seal and contact method conceived for the elevated temperature testing; to get an idea about the general behavior of impedance at elevated temperatures; and to study coarsening effect on stability against sintering.

General behavior of cathode polarization resistance observed thus far, is that, the impedance increases when the dwell time increases at temperatures near or above sintering temperature of cathode, which can is expected from pore closing due to sintering or chemical reaction between LSFC and YSZ. But at lower temperatures, the resistance consistently decreases, one possible reason being a contact problem or insufficient sintering. Also calcined cathode with GDC layer showed a decrease in resistance at 1100°C initially. This initial behavior suggested that the sintering temperature of the cathode samples were perhaps too low and sintering is improving the interface quality at the early stage of accelerated testing. Thus the firing temperature for the above listed anode supported cells were increased to improve the cathode / GDC interface quality.

- Task 3.4 Cell testing with Cr contamination.

One of the key issues regarding the commercialization of low-cost, low temperature solid oxide fuel cell is the use of metallic interconnect. Due to oxidation resistance requirement of such metallic interconnect, this interconnects often contains Cr. However it has been previously demonstrated that the Cr evaporation from Cr oxide scales contaminates the LSM-YSZ cathode triple phase boundary and significantly degrade the performance, [ix] while such Cr contamination affects the LSCF based cathode minimally.[x] Preliminary test on the stability of cell performance was conducted when the cell cathodes are in contact with Cr containing stainless steel, in comparison between LSM-YSZ cathode and LSCF-GDC cathode.

The cell test was performed at 800°C with hydrogen fuel. The initial performance was very steady for both cells (~0.4W/cm^2) up to ~ 50 hours and the cell with LSM cathode started to show some slight drop in power density currently at ~ 70 hours. Further study is required to obtain more meaningful stability data. Note the cells used were from earlier stage of the program and performances were not optimal. Only Ni-YSZ anode supported cells without GDC interlayer were used for this preliminary work

IV. CONCLUSIONS

The summary of the feasibility demonstration study during the phase I period are highlighted below:

- High performance of SOFC's with LSCF-GDC as cathode was demonstrated at 600 °C, on Ni-SDC anode supported cells with ceria electrolyte. Power densities obtained were higher than 1W/cm^2 with cathode polarization resistance as low as 0.16 Ω.cm^2 at 600°C.

- High cell performances were demonstrated for Ni-YSZ anode supported cells with YSZ electrolyte when ceria interlayers were fabricated prior to the LSCF-GDC cathode. The power densities obtained were 1.6 W/cm^2 and 0.8 W/cm^{2}at 800°C and 700°C, respectively. These values are significantly higher than that obtained from Ni-YSZ anode supported cells with YSZ as electrolyte and LSM-YSZ as cathode, with typical power densities of 1-1.1W/cm^2 and 0.5-0.6W/cm^{2}at 800°C at 700 °C, respectively. The performance of cells at 700°C is expected to improve as the processing techniques for the ceria interlayer and the microstructure of cathode are further optimized.

- Symmetric composite cathode samples were used to study the electrochemical reaction at the interface between LSCF-GDC cathode and YSZ electrolyte. With a GDC interlayer between the YSZ and LSCF-GDC layers, the polarization resistance measured at 650°C was 0.3Ωcm^2, more than 50% lower than that without a GDC interlayer. It is suggested that the presence of a ceria diffusion barrier is preventing the formation of a resistive phase resulting from a chemical reaction between LSCF and YSZ during the cathode sintering.

- Basic kinetic data for $La_{0.6}Sr_{0.4}Co_{0.2}Fe_{0.8}O_{3-\delta,}$ were obtained using porous LSCF symmetric samples and Adler-Lane-Steele model.

- A relatively stable performance at 800°C for up to 100 hrs was demonstrated with Ni-YSZ anode supported cells with GDC interlayer. Cathode sintering at much higher temperatures (~1100°C) is possible with GDC interlayer compared without GDC layer (900-950°C). This suggests that the GDC interlayer will considerably improve the long-term stability of the cell. Longer term testing and / or accelerated testing are necessary to better assess the long-term stability of cells using this approach.

The above results suggests the potential of LSCF-GDC cathode for high performance SOFCs operating at 700°C or lower. Notwithstanding the minor adjustments in the tasks list based on the proposal reviewer's comments, all tasks proposed for this phase I project were successfully completed.

V. References

[i]T. Tsai and S.A. Barnett, Solid State Ionics **98,** 191 (1997).
[ii] V. Dusastre and J.A. Kilner, Solid State Ionics, **126** 163 (1999).
[iii] E.P. Murray and S.A. Barnett, Solid State Ionics **148** 27 (2002).
[iv] E. Perry Murray, and S.A. Barnett, in: S.C. Singhal, and M. Dokiya (Eds.), Solid Oxide Fuel Cells VI, The Electrochemical Society Proceedings Series, Pennington, NJ, 1999, p. 369.
[v] Steele, *et al.* Solid St. Ionics 135 (2000) 445
[vi] SA. Adler, J.A. Lane, and B.C.H. Steel, J. Electrochecm. Soc., 143, 3554 (1996)
[vii] S.J. Benson, R.J. Chater, J.A. Kilner, in: T.A. Ramanarayanan et al. (Eds.), Ionic and Mixed Conducting Ceramics III,Vol. 97-24, Electrochemical Society, NJ, 1997, p. 596.
[viii] A. Mai, A.C. Haanappel, F. Teitz, I.C. Vinke and D. Stover, 525, SOFC VIII (2003).
[ix] H.Deng, M.Zhou, and B. Abeles, Solid State Ionics, 74, 75 (1994) ; J. Abel, A.A. Kornyshev, and W. Lehnert, J. Electrochem. Soc., 144, 4523 (1997). ; S.C. Paulson, V.I. Birss, 499, SOFC VIII (2003).
[x] Tokyo Gas Study (2000)